Investigation of luminescent properties of ZnO nanoparticles for their use as a down-shifting layer on solar cells

ARTICLE *in* PHYSICA STATUS SOLIDI (C) CURRENT TOPICS IN SOLID STATE PHYSICS · AUGUST 2013

DOI: 10.1002/pssc.201200950

7 AUTHORS, INCLUDING:

Aleksandra Apostoluk
Institut National des Sciences Appliquées d…
44 PUBLICATIONS **144** CITATIONS
SEE PROFILE

Bruno Masenelli
Institut National des Sciences Appliquées d…
81 PUBLICATIONS **874** CITATIONS
SEE PROFILE

J.-J. Delaunay
The University of Tokyo
112 PUBLICATIONS **927** CITATIONS
SEE PROFILE

Katarzyna Znajdek
Lodz University of Technology
30 PUBLICATIONS **39** CITATIONS
SEE PROFILE

Phys. Status Solidi C **10**, No. 10, 1301–1307 (2013) / **DOI** 10.1002/pssc.201200950

physica status solidi c
www.pss-c.com
current topics in solid state physics

Investigation of luminescent properties of ZnO nanoparticles for their use as a down-shifting layer on solar cells

Aleksandra Apostoluk[*,1], Yao Zhu[1], Bruno Canut[1], Bruno Masenelli[1], Jean-Jacques Delaunay[2], Katarzyna Znajdek[3], and Maciej Sibiński[3]

[1] Université de Lyon, 69000 Lyon, France and INL, CNRS, UMR 5270, INSA Lyon, 69621 Villeurbanne, France
[2] School of Engineering, The University of Tokyo, 7-3-1 Hongo, Bunkyo-ku, Tokyo 113-8656, Japan
[3] Department of Semiconductor and Optoelectronics Devices (DSOD), Technical University of Lodz, ul. Wólczańska 211/215, 90-924 Łódź, Poland

Received 15 November 2012, revised 9 January 2013, accepted 12 March 2013
Published online 13 August 2013

Keywords zinc oxide, nanoparticle, photoluminescence, down-shifting

* Corresponding author: e-mail aleksandra.apostoluk@insa-lyon.fr, Phone: +33 4 72 43 71 86, Fax: +33 4 72 43 85 31

Commercially available solar cells (e.g. CdS/CdTe, CIGS, c-Si) have a spectrally narrow absorption band when compared to the solar emission spectrum. The UV-wavelength response of a solar cell (SC) can be improved by the application of a luminescent down-shifting layer (LDSL) on the SC front side, permitting the conversion of short-wavelength photons to the longer wavelength photons better matching the SC's absorption spectrum. The ideal down-shifting material must possess a large Stokes shift and have a high luminescence quantum yield. We propose the use of the LDSL containing ZnO nanoparticles of less than 5 nm in diameter able to absorb UV light ($\lambda < 400$ nm), where the solar cell spectral response (SR) is low, and re-emitting at longer wavelengths ($\lambda >$ 425 nm), where the typical SC's SR increases. ZnO nanoparticles were synthesized by a low energy cluster beam deposition (LECBD) technique and their luminescent properties were studied as a function of the oxygen partial pressure (OPP) applied during the deposition process. The stoichiometry and crystallinity of ZnO nanoparticles can be controlled via the adjustment of the OPP. It was also observed that there exists an optimal value of the oxygen pressure introduced during the LECBD process, which permits to obtain the highest visible photoluminescence emission, necessary for an efficient down-shifting. The yield of the down-shifting in ZnO nanoparticle layer was determined varying the excitation wavelength using the photoluminescence excitation technique.

1 Introduction The maximum theoretical efficiency of a solar cell (SC) based on a single p-n junction is referred as the Shockley-Queisser limit [1]. It places the maximum solar conversion efficiency at 33.7% for a p-n junction made of a material having a gap of 1.1 eV (like Si). Nevertheless, modern single crystal silicon SCs provide a conversion efficiency of only 27.6% [2]. This value is limited by the optical absorption, surface reflection, carrier transport and carrier collection. Other crucial factors contributing to the limitation of the SC conversion efficiency are: the transparency to the below-bandgap energy photons, radiative recombination and Auger recombination phenomena and the recombination of the excess energy (hot) electrons (which are excited by the above-bandgap energy photons). Only the reduction of these losses can permit the development of more efficient SCs. Figure 1 presents the numerical simulation of a standard c-Si, CdS/CdTe thin-film and CIGS solar cell quantum efficiencies, performed in program SCAPS. The simulations indicate serious quantum efficiency (QE) deficiencies in short wavelength spectrum regions, which may be improved. Various strategies have been proposed to increase the SC conversion efficiency: development of tandem SCs, optical excitation through intermediate bandgap defect levels in order to convert efficiently low energy photons [3], methods for the capture of the infrared light [4] and of the hot electrons or multiple

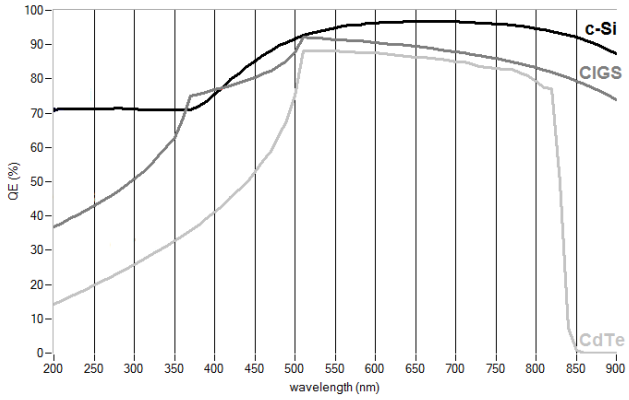

Figure 1 Numerical simulation of a standard c-Si, CdS/CdTe thin films and CIGS solar cells quantum efficiencies (QE), performed in the SCAPS program.

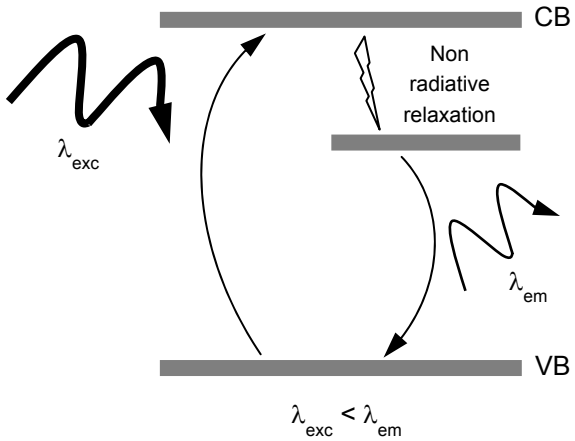

Figure 2 Scheme of the down-shifting process; λ_{ex} is the excitation wavelength; non-radiative relaxation to the defect level in the bandgap via the emission of phonons is shown; the radiative emission from the intermediate energy level at the λ_{em} wavelength follows.

electron generation, fluorescent down-conversion (DC) [5], or thermophotovoltaic DC [6].

The down-conversion is an interesting technique, but difficult to realize as it requires the presence of energy levels exactly in the middle of the bandgap of the down-converting material. One of the strategies permitting to avoid the necessity of the presence of the midgap energy state is the down-shifting (DS) technique. In this process short wavelength (UV) photons are absorbed. The excited electron relaxes non-radiatively to the intermediate energy level state emitting a phonon and then the material reemits photons at longer wavelengths, ideally in the absorption band of the SC, as shown in Fig. 2. In the absence of any competing non-radiative trapping process, the efficiency of such a phenomenon is 100 % (i.e. one absorbed UV photon gives one longer wavelength photon). Photoluminescent down-shifting layers can be placed on a front side of a standard solar cell without any significant modification in the SC's fabrication process. Thus, if the LDSL is used, the SC "sees" the modified incident solar emission spectrum better coinciding with the peak of its spectral response.

The application of semiconducting nanoparticles (NPs) as down-shifters for the enhancement of the SC's spectral response is an interesting issue, as they may possess a high concentration of the intermediate energy levels necessary for efficient DS and can act as an antireflective layer [7]. The NPs for down-shifting should have a strong luminescent emission in the spectral band corresponding to the maximum of the SC's SR, a diameter below 100 nm to avoid strong scattering, be non-hazardous to the environment and human beings and benefit from cheap fabrication techniques. From this point of view, zinc oxide is a very attractive material, as it is a nontoxic, cheap and abundant on Earth. It also benefits from a higher absorption coefficient than other wide bandgap materials such as GaN, as well as easy fabrication methods, which results in lower manufacturing costs of ZnO-based devices. ZnO is typically crystallized in the hexagonal wurtzite structure with possibility of attaining high carrier concentration by the proper material doping. Thanks to these properties ZnO and ZnO:Al (AZO) layers are widely used as transparent contact materials in CIS/CIGS [8], organic [9] and hybrid solar cells applications [10]. ZnO:Al doped layers have been also used as transparent electrode in the silicon SCs [11, 12] and as a refractive index matching layer (antireflective coating) [13].

ZnO is a wide band gap material (~ 3.3 eV at room temperature, corresponding to an absorption wavelength of about 375 nm), close to that of GaN (about 3.4 eV at room temperature). However, ZnO has a larger exciton binding energy than GaN (60 meV, 2.4 times larger than kT at room temperature), which results in bright UV luminescence emission. Perfect crystallinity of ZnO NPs is responsible for the lack of visible luminescence as only the exciton emission is observed. Thus for DS applications, it is necessary to enhance the visible green-red luminescence of ZnO NPs. The luminescent properties of ZnO NPs can be controlled via the adjustment of the NP size and ZnO_x stoichiometry. Indeed, it has been shown that the visible emission in ZnO is also related to crystalline defects (oxygen vacancies…) [14, 15] and that these defects are enhanced as the size is reduced down to the nanoscale. Thus we propose to augment green and red luminescence of the ZnO NPs by deliberate introduction of oxygen defects in the ZnO_x NPs structure and their application as a down-shifting layer in solar cell structures.

Various synthesis methods of ZnO nanostructures exist, such as chemical vapor deposition (CVD), molecular beam epitaxy (MBE) and pulsed laser deposition (PLD). We propose a purely physical method to prepare clusters or cluster assembled nanomaterials called the low energy cluster beam deposition (LECBD) technique [16], as it permits to study the influence of fundamental parameters such as the stoichiometry and the size of ZnO_x NPs on its luminescent properties. However, it should be mentioned that this technique cannot be applied at the industrial scale as it does not permit to deposit large surface layers.

2 Experimental section SCAPS (a Solar Cell Capacitance Simulator) software used to simulate the quantum efficiency of solar cells presented in Fig. 1 is a one dimensional solar cell simulation program developed at the Department of Electronics and Information Systems (ELIS) of the University of Gent, Belgium. The original program was designed for cell structures of the type Cu-$InSe_2$ and CdTe. Recent developments make the program applicable to crystalline solar cells (Si and GaAs) and amorphous cells (a-Si and micromorphous Si). During the simulations all major parameters determining the specific photovoltaic structure are covered. The description of each active layer is realized by the following parameters: E_g (bandgap), χ (electron affinity), ε (dielectric permittivity), N_C (effective density of states in the conduction band), N_V (effective density of states in the valence band), v_{thn} (electron thermal velocity), v_{thp} (hole thermal velocity), μ_n (electron mobility), μ_p (hole mobility), N_A (acceptor density), N_D (donor density), and N_t being the trap (defect) density.

As mentioned above, in the LECBD deposition the NP size, stoichiometry and crystallinity can be adjusted via the control of the deposition parameters such as the nature of the inert gas, the shape and size of the nozzle (see the scheme of the LECBD setup in Fig. 3) and the temperature of the substrate. During the LECBD process, the atomic vapors are generated in high vacuum by Nd-YAG laser evaporation of the target consisting of a stoichiometric ZnO powder (99.99% pure). This powder was beforehand pressed and heated in a furnace at 900 °C under oxygen atmosphere for 8 h. The produced vapors mix with inert rare gas (Ar) introduced at constant speed and lose their kinetic energy via the collisions with the inert gas (plasma quenching), which assures the presence of the nucleation embryos necessary for the formation of neutral clusters. The NPs size essentially depends on the volume of the deposition chamber and the nozzle size. The scheme of the LECBD setup is presented in Fig. 3.
Additional oxygen is injected in the plasma present in the nucleation chamber with different values of the oxygen partial pressure (OPP) when compared to the Ar pressure in order to vary the stoichiometry of the fabricated ZnO_x NPs. The oxygen molecules represent up to 25% of the buffer gas in the nucleation chamber, having a total pressure of 20 mbar.
After the embryos formation in the nucleation chamber, plasma subsequently undergoes a supersonic adiabatic expansion while moving from the nucleation chamber at 20 mbars to the high vacuum deposition chamber at 10^{-7} mbars through a micrometric nozzle, delivering a supersonic jet of clusters with sizes ranging from a few tens to some thousands of atoms (diameters from two to several nanometers). The accretion of the atoms from the plasma onto the embryos takes place in a supersonic nozzle, where the atoms are hyper-quenched beyond the thermodynamic equilibrium and lose their kinetic energy. The preformed clusters are then deposited on a substrate without being shattered, as their kinetic energy per atom is about one order of magnitude lower than the binding energy per atom within the clusters [21] (it is so called "soft landing"). The deposited layer is not continuous and its porosity is of about 70% [17].
The stoichiometry of the ZnO_x deposit can be measured instiu using the X-ray Photoelectron Spectroscopy (XPS) setup installed in the deposition chamber, as shown in Fig. 3.

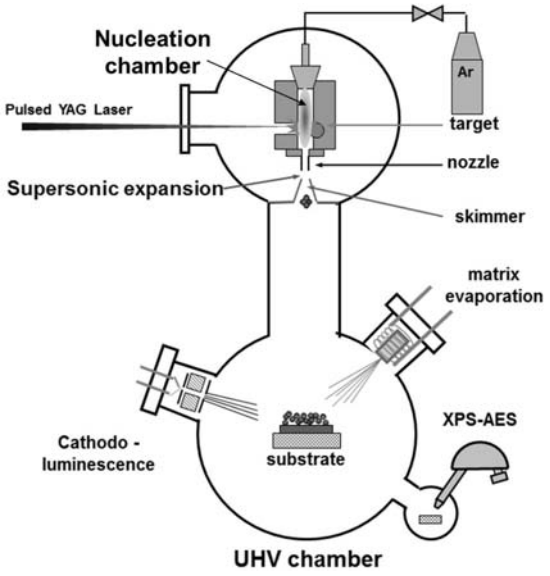

Figure 3 The scheme of the LECBD setup.

The atomic composition and areal mass of the ZnO_x NPs layers were measured ex-situ by Rutherford Backscattering Spectrometry (RBS). The analysis was performed using $4He^+$ ions of 2 MeV energy delivered by the 4 MV Van de Graaff accelerator of the Nuclear Physics Institute of Lyon (IPNL). The backscattered particles were detected with a 13 keV resolution implanted junction set at an angle of 172° with respect to the beam axis. The error of the chemical composition measurement is of ± 2%.

The crystallinity and nanoparticle size are determined from transmission electronic microscopy (TEM) observations. The images are processed with Digital Micrograph software. The crystallinity is deduced from high resolution TEM (HRTEM) images fast Fourier transform (FFT) in the reciprocal space and atomic layout in the direct space.

The room temperature photoluminescence (PL) experiments were performed with a frequency doubled argon laser at 244 nm. The PL signal was dispersed using a Jobin-Yvon HR 640 monochromator using a 600 lines/mm grating blazed at 400 nm and then detected by a GaAs (Hamamatsu H5701-50) photomultiplier. All spectra are corrected to take account for the spectral response of the system and normalized to their maximum.

Photoluminescence excitation measurements (PLE) were performed using the white light from a 100 W tungsten lamp monochromated using the HR 640 monochromator with a 1200 lines/mm grating blazed at 400 nm. This provided excitation wavelengths from 350 to 400 nm range. The photoluminescence emission was collected by a monomode fiber in the 450-650 nm spectral range and analyzed using the iHR320 monochromator with a 600 lines/mm grating blazed at 500 nm and detected by the Si CCD camera cooled with the liquid nitrogen. In all cases the spectra are corrected to take into account the spectral response of the system.

3 Results and discussion The ZnO_x NPs study by transmission electron microscopy (TEM) proved their high crystalline quality and permitted to estimate the NPs size to be less than 5 nm. TEM image of the ZnO_x NP fabricated under the Ar flow presented in Fig. 4 shows a crystal with atomic rows clearly visible (left-side image). The right-side image in Fig. 4 is the FFT of HRTEM image viewed along the [01-10] zone axis, revealing that the nanoparticles are crystallized in the wurtzite phase, with the reflections from (0002) and (10-11) planes clearly identified.

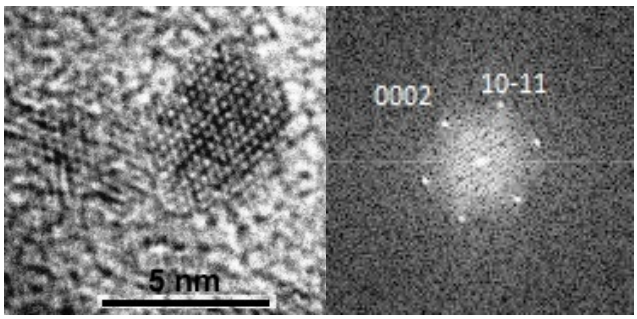

Figure 4 Left: HRTEM images of the ZnO NPs obtained with the LECBD method under the argon flow; the size of one ZnO nanoparticle is less than 5 nm. Right: FFT of the ZnO nanoparticle viewed along the [01-10] zone axis. The (0002) and (10-11) planes of the wurtzite structure are unambiguously identified.

It was observed that depending on the method of the incorporation of oxygen into the ZnO_x NPs, post deposition exposition of the clusters to the oxygen or the introduction of the oxygen in the nucleation chamber, the obtained nanoparticles with identical stoichiometry exhibit very different luminescent properties [18]. The cathodoluminescence studies showed that the post-deposition oxygen addition does not significantly improve the green-red luminescence of the ZnO_x NPs, as it influences neither their stoichiometry, nor the crystalline quality [18]. On the contrary, the addition of the oxygen to the inert gas in the nucleation chamber improves the stoichiometry in a spectacular way. No metallic contribution to the Auger spectra was observed on the ZnO_x clusters obtained with different partial pressures of the oxygen and the spectra looked like these of pure ZnO_x (without metallic Zn) [18].

Thus to obtain the non-stoichiometric ZnO_x NPs with efficient green-red luminescence (necessary for DS), it is required to vary the oxygen partial pressure in the plasma in the nucleation chamber during the LECBD.

ZnO_x NPs thin layer (several tenths of nm) were deposited under various oxygen partial pressures: 25% of the buffer gas (the OPP was equal to 5 mbar), 12.5% (the OPP = 2.5 mbar) and 7 % of the buffer gas (the OPP = 1.4 mbar). The corresponding stoichiometry of the ZnO_x was estimated with the calibrated XPS measurement. The x for the OPP of 5 mbar results in stoichiometric ZnO_x NPs, x = 1, the one of 2.5 mbar and 1.4 mbar give the non-stoichiometric ZnO_x, with nominal values of x = 0.5 and 0.28, respectively. The OPP values above 25 % of the buffer gas pressure in the nucleation chamber do not improve the ZnO_x stoichiometry in a significant manner [18].

The stoichiometry of the fabricated ZnO_x NPs was measured by Rutherford Backscattering Spectrometry (RBS), some days after their deposition and exposition to the ambient air. The measurements using this technique showed that all ZnO_x NPs layers studied are stoichiometric (x = 1), though for the OPP of 2.5 mbar and 1.4 mbar used in the LECBD the resulting ZnO_x NPs should be non-stoichiometric (i.e. contain oxygen vacancies). In the example of the RBS spectrum shown in Fig. 5, the expected oxygen content was x = 0.28, as measured with the XPS in the LECBD deposition chamber and the RBS measurement yielded x = 1. Thus it is believed that the NPs layer adsorbed oxygen and water molecules from the ambient atmosphere. The high roughness of the ZnO_x NPs film, which can be evidenced from the low energy tail of the RBS signal from Zn in Fig. 5, supports the hypothesis of an enhanced chemical reactivity of the deposit.

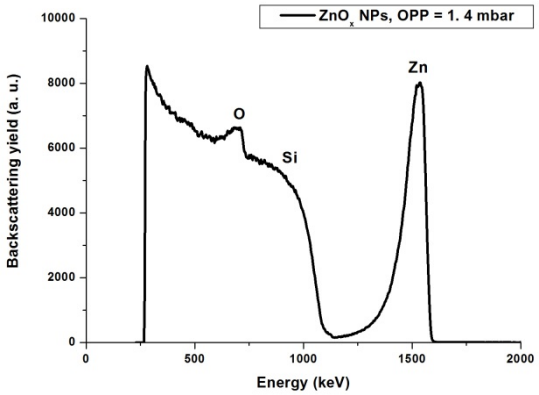

Figure 5 RBS spectrum recorded on ZnO_x NPs with a nominal value x = 0.28, deposited under the OPP of 1.4 mbar. Within the experimental uncertainties, the deposit is stoichiometric (measured value: x = 1) and its areal mass is 66 µg cm^{-2}. *Analysis conditions:* $^4He^+$ ions of 2 MeV energy; detection angle of 172°.

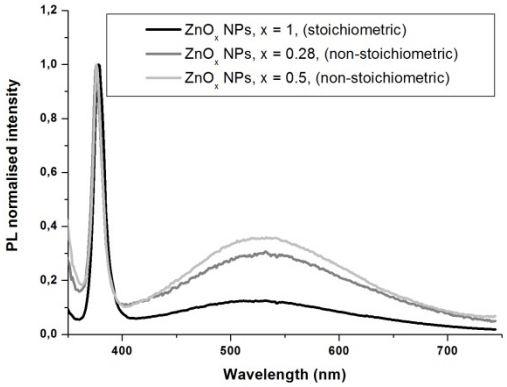

Figure 6 Room temperature photoluminescence of the ZnO_x NPs as function of their stoichiometry. It can be clearly noticed that the maximum visible PL is observed for the nominal stoichiometry of x = 0.5.

Then the PL spectra of the fabricated ZnO_x NPs layers were measured. As shown in Fig. 6, two contributions to the PL signal are observed for all samples – the near band edge emission and the green-red luminescence peak. In non-stoichiometric ZnO_x NPs, the increase of the green and red emission can be observed, to the detriment of the excitonic emission. The near band edge contribution is located at 378 nm as already observed for other ZnO nanostructures at room temperature. The defect-related green-red luminescence band in our case is centered at around 530 nm and its origin is still controversial. The most commonly evoked hypothesis explains the origin of this emission band from the presence of singly ionized oxygen vacancies and zinc interstitials, though other theories suggesting the contamination with OH groups have been proposed [19-21].

It should be noted that the ratio between the two contributions, i.e. the excitonic and the visible emission is often used as an indirect probe of ZnO film crystalline quality.

It was reported that the incorporation of the atomic oxygen during the cluster growth by LECBD permits to avoid the formation of the native defects in the grown nanoparticles [18]. Thus the decrease of the OPP value below 25% of the buffer gas pressure in the LECBD process should lead to the ZnO_x NPs with a poor crystallinity and increase the green-red luminescence of the fabricated NPs. It is observed that the PL signal for ZnO_x depends on the OPP value applied during the LECBD, as presented in Fig. 6. It can be clearly noticed that the visible luminescence of the ZnO_x NPs having the nominal value of x = 1 (as measured with the XPS in the LECBD deposition chamber) was much lower than the green-red luminescence from films having x = 0.5 (25% of oxygen in the buffer gas) and x = 0.28 as nominal value (7% of oxygen in the buffer gas).

This is not surprising, as for x = 1 the ZnO_x NPs are perfectly stoichiometric, having a good crystalline quality with no defects. More unexpectedly, the ZnO_x NPs deposited under the OPP of 2.5 mbar in the nucleation chamber (12.5% of the buffer gas) give higher visible luminescence emission than the ZnO_x NPs deposited under the OPP of 1.4 mbar in the nucleation chamber (7% of the buffer gas). It can be concluded that the ratio between the visible and UV luminescence of the ZnO_x NPs is not linear in function of x and that there exists an optimal OPP in the buffer gas injected during LECBD, which permits to obtain the highest green-red luminescence. We suppose that too low OPP (below 5 mbar in the buffer gas) leads to the formation of the ZnO_x NPs of too poor crystalline quality with many oxygen vacancies in the crystal structure, which may be detrimental to the luminescent activity.

Strong green-red emission is profitable for the DS process as it is a proof that the material absorbs the UV light and emits the visible light efficiently via a down-shifting mechanism. In order to confirm this statement, we performed the PLE on the nonstoichiometric ZnO_x NPs for which x = 0.5 (deposited under 12.5% oxygen in the buffer gas). The results are presented in Fig. 7. It can be clearly noticed that the total luminescence intensity is observed in the spectral range between 360-370 nm, which confirms that the material absorbs the UV light and reemits photons at longer wavelengths.

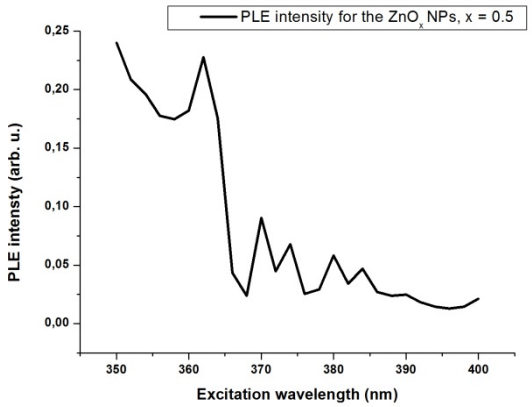

Figure 7 The PLE spectrum (integrated intensity between 450 and 650 nm) of the ZnO_x NPs with the nominal value x = 0.5 (as measured with the XPS in the deposition chamber) as function of the excitation wavelength.

All ZnO NPs films were exposed to the ambient air after deposition and as they are very porous (the porosity is of about 70%), oxygen molecules adsorbed on the NPs surface. This surface adsorption enhances the green-red luminescence emission, which is also beneficial for the efficient DS.

4 Conclusions and perspectives ZnO_x nanoparticles fabricated using the LECBD method were grown and their structure, composition and RT photoluminescence properties were studied. It was demonstrated that the ratio between the excitonic and the visible photoluminescence (PL) emission band can be adjusted via the oxygen pressure applied during the LECBD of the ZnO_x NPs. It was observed that higher oxygen pressure leads to higher content of the oxygen in the structure of ZnO_x NPs and that for the OPP of 25% the drastic decrease of the green-red photoluminescence signal is observed. This is obtained for OPP equal or above 25% in the buffer gas. It is attributed to better crystalline quality of the stoichiometric ZnO_x, as the oxygen introduced directly in the nucleation chamber during the LECBD permits to avoid the formation of native defects in the clusters, leading to well crystallized particles with nanometric sizes.

It is also clearly demonstrated that there exists an optimal value of the OPP during the LECBD which permits to obtain the highest visible PL emission, necessary for the efficient DS. As observed, it is not the lowest OPP which gives the ZnO_x NPs with most intense green-red PL emission, as too poor crystalline quality leads to the quenching of the visible PL. The effect of the exposition of the ZnO_x NPs to the ambient air on the green-red PL intensity was studied and it was observed that it increases for the ZnO_x NPs fabricated under OPP of 12.5%, the ones which give the highest visible PL emission, though the reasons of this phenomenon remain inexplicable up to date.

The RBS studies of the ZnO_x NPs fabricated under various OPP indicate that all these NPs are stoichiometric, contrary to the values of the oxygen content measured with the XPS installed in the deposition chamber. We conclude that the deep defect levels generate free electrons that are trapped at the NP surface by oxygen adsorption.

A ZnO_x NP layer with optimized stoichiometry can be used as a luminescent converter placed on the front surface of any SC, as it has the advantage of being applicable to any existing SC structure. Ongoing work aims to quantify precisely the amount of the UV photons converted into green-red photons by a ZnO_x NP and validate its application as a luminescent down-shifting layer in solar cell structures.

Acknowledgements The studied ZnO nanoparticles were fabricated using the facilities of the PLYRA (Plateforme LYonnaise de Recherche sur les Agrégats) platform at the Lyon 1 university. The authors gratefully acknowledge Olivier Boisron and Dimitri Hapiuk for their assistance in the ZnO nanoparticles layer deposition and Karine Masenelli-Varlot and Centre LYonnais de Microscopie (CLYM platform) for making TEM images.

References

[1] W. Shockley and H. J. Queisser, J. Appl. Phys. **32**, 510 (1961).
[2] M. A. Green, K. Emery, Y. Hishikawa, W. Warta, and E. D. Dunlop, Prog. Photovolt.: Research and Applications, **20**, 606 (1912), Special Issue: Adventures in Cu-Chalcogenide Solar Cells.
[3] A. S. Brown and M. A. Green, J. Appl. Phys. **92**, 1329 (2002).
[4] B. Jalali, S. Fathpour, and K. Tsia, Opt. Photon. News **20**, 18 (2009).
[5] B. S. Richards, Sol. Energy Mater. Sol. Cells **90**, 1189 (2006).
[6] N.–P. Harder and P. Würfel, Semicond. Sci. Technol. **18**, S151 (2003).
[7] Z. R. Abrams, A. Niv, and X. Zhang, J. Appl. Phys. **109**, 114905 (2011).
[8] S. Park, T. Ikegami, and K. Ebihara, Thin Solid Films **513**, 90 (2006).
[9] K. Ramanathan, M. A. Contreras, C. L. Perkins, S. Asher, F. S. Hasoon, J. Keane, D. Young, M. Romero, W. Metzger, R. Noufi, J. Ward, and A. Duda, Prog. Photovolt.: Research and Applications **11**, 225 (2003).
[10] M. White, NNIN REU Research Accomplishments (2005), pp. 156–157.
[11] Z. C. Zin, I. Hamberg, and C. G. Granqvist, J. Appl. Phys. **64**, 5117 (1988).
[12] M. Sibiński, K. Znajdek, S. Walczak, M. Słoma, M. Górski, and A. Cenian, Mater. Sci. Eng. B **177**, 1292 (2012).
[13] Y.–J. Lee, D. S. Ruby, D. W. Peters, B. B. McKenzie, and J. W. P. Hsu, Nano Lett. **8**, 1501 (2008).
[14] A. Janotti and C. G. Van de Walle, Rep. Prog. Phys. **72**, 126501 (2009).

[15] I. Musa, F. Massuyeau, L. Cario, J. L. Duvail, S. Jobic, P. Deniard, and E. Falques, Appl. Phys. Lett. **99**, 243107 (2011).
[16] A. Perez, P. Mélinon, V. Dupuis, P. Jensen, B. Prevel, J. Tuaillon, L. Bardotti, C. Martet, M. Treilleux, M. Broyer, M. Pellarin, J. L. Vaille, B. Palpant, and J. Lerme, J. Phys. D: Appl. Phys. **30**, 709 (1997).
[17] D. Tainoff, PhD thesis, Influence des défauts sur les proprié tés optiques et électroniques des nanoparticules de ZnO, (Université Claude Bernard Lyon I, Lyon, 2009).
[18] D. Tainoff, B. Masenelli, O. Boisron, G. Guiraud, and P. Mélinon, J. Phys. Chem. C **112**, 12623 (2008).
[19] Ü. Özgür, Y. I. Alivov, C. Liu, A. Teke, M. A. Reshchikov, S. Doğan, V. Avrutin, S.-J. Cho, H. Morkoç, J. Appl. Phys. **98**, 041301 (2005).
[20] A. B. Djurišić and Y. H. Leung, Small **8-9**, 944 (2006).
[21] N. S. Norbert and D. R. Gamelin, J. Phys. Chem. B **109**, 20810 (2005).